

Robustness of WDM technique for the co-propagation of quantum- with classical signals in an optical fiber

Sumit Chaudhary, Shahram Dehdashti, Igor Litvin, Janis Nötzel
Emmy-Noether Group Theoretical Quantum Systems Design
Technical University of Munich
Munich, Germany
{sumit.chaudhary, shahram.dehdashti, igor.litvin, janis.noetzel}@tum.de

Abstract—Many quantum communication systems operate based on weak light pulses which by design are assumed to operate in isolation from regular data traffic. With the widespread availability and commercialization of these systems comes a need for seamless integration already at the physical layer. In particular for optical fiber links where wavelength division multiplexing (WDM) is the dominant data transmission technique this results in the propagation of very weak quantum signals against a strong data signal background. With this work, we present a novel theoretical approach that studies the evolution of co-propagating quantum and classical signals that are launched using WDM. The important factors that contribute to crosstalk, such as the launch power of the classical signal and the separation between the two signals in terms of wavelength, are comprehensively analyzed. Interestingly, calculations show that only the first two nearest channels from the classical channel experience noticeable crosstalk whereas other distant channels have negligible crosstalk effect. This reflects the WDM technique is in principle robust in the integration of weak quantum links into classical data traffic.

Index Terms—crosstalk, quantum optics, quantum key distribution, optical fiber, nonlinear Schrödinger equation

I. INTRODUCTION

Optical fiber is the backbone of present-day communication systems and also a key component for the transmission of quantum states. Due to the dependence of free-space optical links on weather conditions, optical fiber links will continue to be an important ingredient to the commercialization of these new communication technologies and paradigms. Recent advances in the development of quantum technology range from Quantum Key Distribution (QKD) [1], [2], quantum secret sharing [3], [4], authentication [5], quantum digital signatures [6], etc.

Continuous-Wave (CW) lasers are a widely used coherent source as a carrier of quantum information. These coherent states are the technological basis for present-day data transmission systems. Experimentally, optical pulses are directly generated from a mode-locked laser or an externally used intensity modulator to convert the CW laser field to an optical pulse. Since an optical pulse has finite temporal width it

necessarily has finite bandwidth in the frequency domain and is therefore best described as a multi-mode coherent state [7]. While in this work a mode refers to a frequency of the optical field, quantum communication experiments are utilizing a multitude of different physical degrees of freedom as well. For example, these are polarization [8], time-bin [9] or phase encoding [10]–[12] which are all based on optical pulses to encode quantum information. Owing to the simplicity of the BB84 protocol [13] which is based on the primitive of conjugate coding [14], QKD technology is already at a very high technological readiness level, with commercial devices available and ready to implement to secure communication networks. The quantum states used in QKD and other quantum communication paradigms are all based on the use of extremely low-intensity optical pulses at single photon levels and are therefore typically designed for use on dark fibers, where the noise background is minimal. The different realizations of quantum communication protocols all come along with several advantages and disadvantages. Here, we point out the stability of phase encoding and time-bin coding on optical fiber in comparison to polarization encoding, which often times suffers from environmental stress via birefringence and the resulting polarization drift. In implementation, quantum technology services such as QKD must however compete against cost-effective solutions like [15] and [16]. With this in mind, low-cost integration into the existing physical layer and co-existence with classical data channels become mandatory. For example, these can use wavelength division multiplexing. However, as pointed out above, all known implementations of QKD systems operate with extremely low intensities compared to classical data channels, crosstalk can therefore severely deteriorate the QKD operation. Thus a careful selection of input launch power and wavelength separation between the two signals must be practiced to provide required isolation to the quantum signals to efficiently coexist alongside the classical data traffic. These effects of launch power and wavelength separation are the key investigation subjects of this article. We study the crosstalk as the distortion in the quantum signal when it is co-propagating with the classical data traffic.

In the following, we briefly review several reports on

This work was financed by the DFG via grant NO 1129/2-1 and by the BMBF via grants 16KISQ168, 16KISQ077, 16KISR02 and 16KISQ0396.

successful integration of QKD- and classical data transmission services. In [17], the quantum signal is launched in the O-band at 1310 nm and classical data in the C band to preserve the quantum signal from Raman scattering. In [18] both quantum and classical signals are in the C-band to share a secret key over 50 km. Secret key generation with QKD protocols using weak coherent pulses that were sent with classical data traffic in the C-band was demonstrated in [19], [20], [21]. In other experiments, continuous variable (CV) QKD has been demonstrated with classical 100 WDM channels [22]. In recent years, integration of QKD with state-of-the-art data traffic has been demonstrated by integrating with high classical data traffic [23], [24].

It can be deduced from the literature, that the use of a common fiber link for QKD and classical data traffic requires careful selection of wavelength separation between signals, peak input power, optical pulse width and highly depends on the type of encoding in QKD protocol. In this work, we will therefore for the first time theoretically investigate crosstalk in the quantum mechanical framework in a case where weak laser pulses are used for quantum communication.

Outline- In Section II, we describe the quantum theory of pulse propagation in optical fiber. In Section III, a formalism is developed to narrate crosstalk. Then, Section IV comprises theoretical findings to understand the crosstalk behavior in various scenarios. We describe the numerical methods used in this work in Section V. This work is concluded in Section VI.

II. PULSE PROPAGATION IN OPTICAL FIBER

The propagation of an optical field inside an optical fiber is most accurately characterized by the generalized nonlinear Schrödinger equation (GNLSE). The equation provides a comprehensive description of the optical pulse's evolution, encompassing various phenomena such as attenuation, group velocity dispersion, and nonlinear effects including the Kerr effect, Stimulated Raman scattering (SRS), and Stimulated Brillouin scattering (SBS). This theory was subsequently refined within the framework of quantum mechanics to describe the propagation of quantum optical pulses propagating inside optical fibers [25]–[27]. A Hamiltonian can be constructed for the optical fiber by considering a Kerr medium which is coupled to the photon gain/loss reservoir and that is also coupled to the phonon reservoir to incorporate the Stimulated Raman Scattering (SRS), is given as [25]:

$$\hat{H} = \hat{H}_F + \hat{H}_{NL} + \hat{H}_R + \hat{H}_S. \quad (1)$$

here, \hat{H}_F is the Hamiltonian for the free energy of the electromagnetic field in a linear dispersive medium, \hat{H}_{NL} accounts for energy due to the intensity-dependent Kerr effect. The term \hat{H}_R is the energy of the phonon reservoir and its coupling with electromagnetic field modes that are responsible for SRS. Similarly, \hat{H}_S is the energy of the photon scattering reservoir and its coupling with electromagnetic field modes

accounting for the photon loss in the medium. The photon field operator $\hat{\alpha}$, peaked at wavenumber k_0 is defined as

$$\hat{\alpha}(z, t) = \frac{1}{\sqrt{2\pi}} \int dk \hat{a}(k, t) e^{i((k-k_0)x + i\omega_0 t)} \quad (2)$$

with the commutation relation $[\hat{\alpha}(z, t), \hat{\alpha}^\dagger(z, t')] = \delta(z - z')\delta(t - t')$.

By using the positive-P representation, in which the density matrix is defined as

$$\hat{\rho}(t) = \int P(t, \alpha_1, \alpha_2) \frac{|\alpha_1\rangle\langle\alpha_2|}{\langle\alpha_1|\alpha_2\rangle} d^2\alpha_1 d^2\alpha_2, \quad (3)$$

the GNLSE leads to Fokker Planck equation with positive definite diffusion coefficients that can be equivalently written in the form of coupled stochastic differential equations in scaled field operators $\phi(z, t)$ and $\phi^+(z, t)$, i.e.,

$$\frac{\partial\phi}{\partial\zeta} = -\frac{i}{2}[1 \pm \frac{\partial^2}{\partial\tau^2}]\phi + i\phi^+\phi^2 - \gamma\phi + \xi_L + \sqrt{i}\xi_E\phi \quad (4a)$$

$$\frac{\partial\phi^+}{\partial\zeta} = \frac{i}{2}[1 \pm \frac{\partial^2}{\partial\tau^2}]\phi^+ - i\phi\phi^{+2} - \gamma\phi^+ + \xi_L^+ + \sqrt{-i}\xi_E^+\phi^+ \quad (4b)$$

where $\zeta = z/L_d$ is the distance along the fiber in units of characteristic length scale called dispersion length, denotes $L_d = t_0^2/|\beta_2|$, in which β_2 is the dispersion coefficient of the fiber; the sign of dispersion coefficient, for normal dispersive medium is positive while for anomalous dispersive medium is negative that supports the formation of optical solitons; moreover, $\tau = (t - z/v_g)/t_0$ is the scaled time, in which v_g denotes the group velocity of the optical field. The attenuation of the field inside the fiber is denoted by γ having value $2.3 \times 10^{-5}L_d$ corresponds to 0.2 dB/km in the wavelength region around 1550 nm. Since this work does not include sub-picosecond pulses or fields with a broad spectrum Raman scattering is neglected. ϕ and ϕ^+ used in (4) are obtained from scaling phase space variables as following:

$$\phi(\zeta, \tau) = \sqrt{\frac{v_g t_0}{n_0}} \alpha_1(\zeta, \tau) \quad (5a)$$

$$\phi^+(\zeta, \tau) = \sqrt{\frac{v_g t_0}{n_0}} \alpha_2(\zeta, \tau). \quad (5b)$$

In above expression $n_0 = t_0/(\hbar\omega_0 L_d \gamma_{nl})$. $\xi_L(\zeta, \tau)$ and $\xi_L^+(\zeta, \tau)$ are complex-valued stochastic noise arising from attenuation of photons inside fiber whereas $\xi_E(\zeta, \tau)$ and $\xi_E^+(\zeta, \tau)$ are real-valued stochastic noise due intensity dependent Kerr nonlinearity. These two stochastic fields obey the following correlation

$$\langle \xi_L(\zeta, \tau) \xi_L^+(\zeta', \tau') \rangle = \frac{2\gamma n^{th}}{n_0} \delta(\zeta - \zeta') \delta(\tau - \tau') \quad (6)$$

$$\langle \xi_E(\zeta, \tau) \xi_E^+(\zeta', \tau') \rangle = \frac{1}{n_0} \delta(\zeta - \zeta') \delta(\tau - \tau') \quad (7)$$

Cross-correlation between ξ_E and ξ_E^+ vanishes and auto-correlations of ξ_L and ξ_L^+ is zero [25]. Here, $n^{th} = (\exp[\hbar\omega_0/k_B T] - 1)^{-1}$ is the thermal occupation number for the bosonic reservoir.

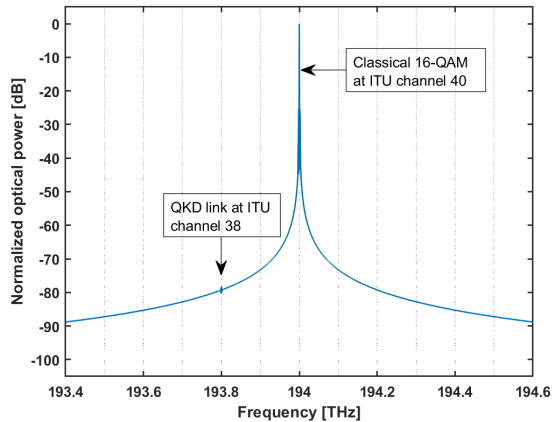


Fig. 1. Illustration of co-propagating quantum and classical signal in a wavelength division multiplexing system utilizing c-band. Vertical lines in the background are standard ITU channels with 100 GHz spacing. From the spectrum, the power difference between the two signals is visible when they are separated by 200 GHz.

III. CROSSTALK BETWEEN QUANTUM AND CLASSICAL SIGNAL

In the context of this paper, we distinguish classical and quantum signals based on their application. Although both are generated from lasers, a classical signal refers to an optical field used for classical communication applications whereas a quantum signal refers to an optical pulse that is the carrier of quantum information in some quantum communication protocols like QKD. Depending upon the nature of the quantum source of light there may exist a variety of quantum optical states but the analysis in this paper is limited to the weak optical pulses considered as multimode coherent state. The term multimode is necessary to emphasize because an optical pulse of finite duration consists of several frequency modes by Fourier transform property. In the case of QKD, these weak optical pulses carry quantum information encoded in phase, polarization, or the relative time of arrival of photons. Classical data transmission in optical fiber utilizes different optical frequencies in wavelength division multiplexing (WDM). The total power of these signals is usually on a milliwatt scale whereas a quantum signal has power at the nanowatt level or even below in the single photon regime. An optical field that is launched inside the fiber undergoes group velocity dispersion (GVD) that temporally broadens an optical pulse depending on the dispersion coefficient β_2 and the initial pulse width t_0 . The nonlinear Kerr effect arising from the third-order nonlinear susceptibility $\chi^{(3)}$ is power dependent which gives rise to self-phase modulation and cross-phase modulation effects. We start our crosstalk analysis by assuming a WDM system whose j^{th} channel is centered at carrier frequency ω_j and channels have uniform frequency spacing $\Delta\omega$. A quantum signal is defined as a weak coherent pulse with a temporal width t_0 and average photon number μ centered at frequency ω_q . We assume a 16-QAM classical signal that can be mathematically constructed using a random sequence of

constellation symbols at a bit transfer rate R_c . The Inphase and Quadrature components of QAM are prepared using a root-raised cosine filter and are mixed together with the carrier frequency. The detailed description of QAM can be found in [28]. The scaled amplitude of the overall classical and quantum signal launched into the optical fiber using a WDM can be written as:

$$\phi(0, \tau) = \sqrt{\gamma_{nl} L_d} \left[\sqrt{P_0} Q(\tau) e^{i\Omega_j \tau} + \sqrt{\frac{\hbar\omega_q \mu}{t_0 \sqrt{\pi}}} e^{-\frac{\tau^2}{2t_0^2}} e^{i\Omega_q \tau} \right] \quad (8)$$

and $\phi^+(\zeta = 0, \tau) = \phi^*(\zeta = 0, \tau)$. In the above equation, the first term represents the classical 16-QAM signal with launch power P_0 and launched into channel j and second term is the Gaussian pulse representing the quantum signal with average photon number μ in channel q of the WDM system. Since, we are working in the scaled coordinate ζ and τ , so $\Omega_j = \omega_j t_0$ and $\Omega_q = \omega_q t_0$. $Q(\tau)$ is the waveform of the classical 16-QAM signal. The spectrum of such an initial state is shown in Fig. 1. As the field propagates inside the fiber the interaction between these two signals is governed by (4a) and (4b). At the end of the optical fiber, the quantum signal is recovered from the DWM system by only selecting the spectral modes of the quantum channel. The recovered quantum signal from the optical fiber can be calculated as follows:

$$\phi_q\left(\frac{L}{L_d}, \tau\right) = \frac{1}{2\pi} \int_{\Omega_q - \frac{\Delta\omega}{2}}^{\Omega_q + \frac{\Delta\omega}{2}} \left[\int_{-\infty}^{\infty} \phi\left(\frac{L}{L_d}, \tau\right) e^{-i\omega\tau} d\tau \right] e^{i\omega\tau} d\omega. \quad (9)$$

Similarly, $\phi_q^+(L/L_d, \tau)$ can be calculated and the intensity of the output optical pulse is calculated as $\phi_q \phi_q^+$.

One qualitative way of defining crosstalk is to calculate the distortion in the intensity of the quantum signal during co-propagation. Let us say $\tau_{RMS}^{(co)}$ is the root mean square (RMS) width of the quantum signal when multiplexed with the classical signal using WDM and $\tau_{RMS}^{(df)}$ is the RMS width of the quantum signal propagating in dark fiber alone. Then the crosstalk $\mathcal{C}(\zeta)$ is defined as the ratio of these two RMS widths.

$$\mathcal{C}(\zeta) = \frac{\tau_{RMS}^{(co)}}{\tau_{RMS}^{(df)}} \quad (10)$$

A value of $\mathcal{C}(\zeta) \approx 1$ implies that the quantum signal is sufficiently isolated from the classical signal and experiences no crosstalk similar to the dark fiber usage. A value of $\mathcal{C}(\zeta) > 1$ indicates a large extent of impairments to the quantum signal.

IV. RESULTS

We numerically solve the coupled stochastic differential equation (4) using the parameters of the SMF 28 optical fiber. We consider a 100 GHz spacing grid as per the International Telecommunication Union (ITU) standard, where the classical and quantum signals are placed in the C-band, which spans from 1530 nm to 1565 nm including 44 WDM channels from ITU channel no 16 to 59. All these channels are assumed to have same attenuation coefficient of 0.2 dB/km. All parameters

TABLE I
INPUT PARAMETERS

Parameter	symbol	value
Pulse duration	t_0	$\sqrt{2} 100 \text{ ps}$
WDM channels spacing	$\Delta\omega$	$2\pi 100 \text{ GHz}$
Average photon number in quantum signal	μ	0.4
Temperature	T	300 K
Fiber length	L	50 km
Kerr nonlinear coefficient	γ_{nl}	$0.78 \text{ W}^{-1} \text{ km}^{-1}$
Dispersion coefficient	β_2	$-18 \text{ ps}^2/\text{km}$
Bit transfer rate (16-QAM)	R_c	10 Gbps

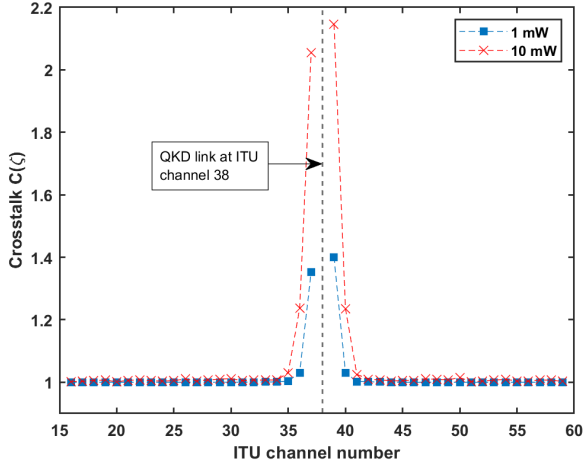


Fig. 2. Crosstalk \mathcal{C} is calculated by fixing the quantum signal in ITU channel 38 (1546.92 nm) and varying classical channel all over the C-band from ITU channel 16 to 59.

utilized in the calculation are listed in Table I. The quantum signal is assigned ITU channel 38 and the classical channel is varied from channel no. 16 to 59 to cover all the C-band with two different power levels of 1 mW and 10 mW as shown in Fig. 2. In the figure, we quantify the reduction of crosstalk when the classical communication channel is set to ITU channel 39 as compared to ITU channel 40. We observe that setting the classical channel above ITU channel 40 or below 36 leads to a very good isolation of the quantum channel. It is clearly visible that when these two signals are separated by at least two empty channels in between, crosstalk is almost negligible with $\mathcal{C}(\zeta)$ approximately equal to 1.

When the classical channel is chosen adjacent to the quantum channel, i.e. ITU channel 37 or 39, a significant crosstalk is observed that is power dependent. The crosstalk is reduced as the wavelength separation increases i.e. classical channel as ITU 36 or 40. This crosstalk characterization which is power-dependent and depends on wavelength separation, demonstrates the robustness of the WDM technique for the co-propagation of quantum and classical signals in the same fiber. This theoretical result clearly states that QKD technology is compatible with service fibers using the WDM method and has the potential to be integrated with the standard telecommunication infrastructure.

Since the classical channel adjacent to the quantum channel

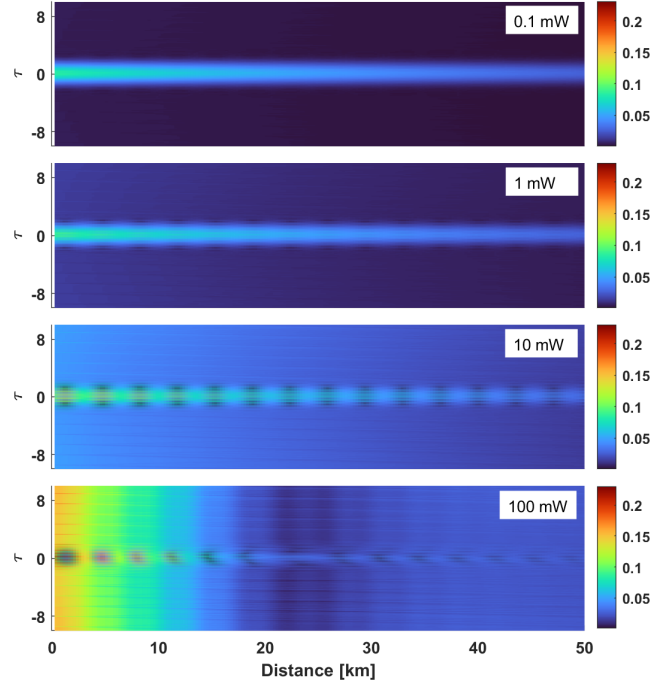


Fig. 3. Propagation of optical pulse representing the quantum signal in the fiber. τ is the time scale in units of pulse width in the moving frame of reference. These density plots present the quantum signal at ITU channel 38 (1546.92 nm) while the classical channel is adjacently placed in ITU channel 39 (1546.12 nm) and the launch power is varied from 0.1 mW to 100 mW.

incurs maximum crosstalk we further analyze the case when the classical signals are sent in ITU channel 39 and 40 whereas the quantum signal lies in ITU channel 38. In Fig. 4 the input launch power of the classical signal is varied from 0.1 mW to 100 mW and the crosstalk is depicted. As can be expected, the crosstalk increases monotonically with the power of the classical signal.

In Fig. 3 we display the temporal power distribution in a frame moving with the quantum signal over the length of the fiber to visualize the increase distortion caused by high power classical signals with their energy. Only spectral components corresponding to ITU channel 38 where the quantum signal is operated contribute to the energy displayed in the figure.

We then further investigate the effect on crosstalk by reducing the temporal pulse width (t_0) of the quantum signal. In practical applications like QKD, a train of optical pulses is generated instead of a single pulse and to achieve a high key rate, it is preferred to generate these pulses at a high repetition rate [11], [29]–[31] by reducing the pulse temporal width. In the corresponding Fig. 5 crosstalk is calculated by narrowing the pulse width but the average photon number μ is kept constant. Calculations show that the crosstalk decreases as the pulse shrinks in temporal width. We attribute this behaviour to the fact that for a wavepacket of constant energy, a reduction in the temporal width will increase the optical power. This increment in power reduces the power difference between classical and quantum signals hence achieving a crosstalk

reduction. We deduce that higher clock speed QKD systems will perform better in a WDM system with classical data traffic. However, our analysis is limited in two aspects: First, when the pulse width reduces to subpicosecond size then Stimulated Raman scattering [32] cannot be neglected and a careful approach is required to estimate crosstalk. Second, the increase in spectral width will at some point lead to an increase in crosstalk, letting us speculate about the existence of a sweetspot of temporal width at which the minimum crosstalk at maximum key rate is reached.

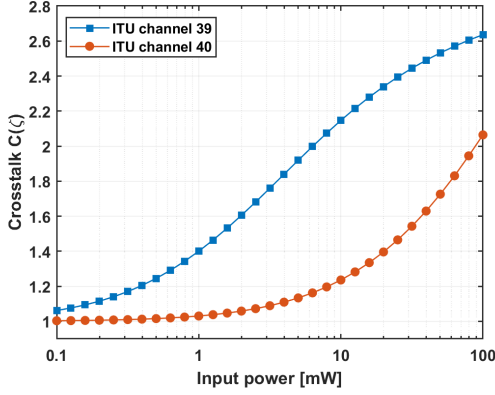


Fig. 4. Crosstalk effect when the classical channel is placed close to the quantum channel. The launch power is varied while the quantum channel is kept fixed at ITU channel 38 with an average photon number 0.4 and temporal pulse width $t_0 = \sqrt{2}$ 100 ps.

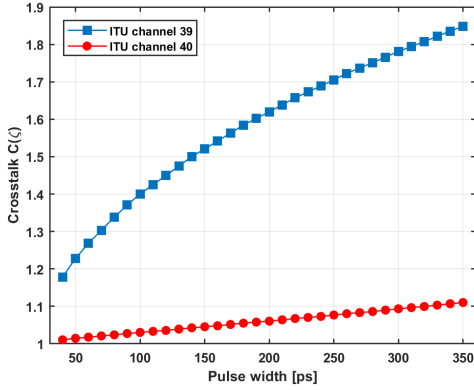


Fig. 5. Effect of optical pulse width of the quantum signal on the crosstalk. The input power of the classical signal is 1 mW and the quantum signal lies in ITU channel 38.

V. METHODS

Split step Fourier method [33], [34] is the most preferred method to solve classical NLS equation for optical fiber. Here, in the quantum version there are two coupled equations with stochastic noise we use the Ito semi-implicit midpoint method [35]. Numerically, $\phi(\zeta, \tau)$ and $\phi^+(\zeta, \tau)$ evolve in step of $\Delta\zeta$

such that $\zeta_{n+1} - \zeta_n = \Delta\zeta$ is the step size along propagation direction. Equation (4a) can be rewritten as:

$$\frac{\partial\phi}{\partial\zeta} = \mathbf{L}\phi + \mathbf{N} \quad (11)$$

here, \mathbf{L} is a linear operator and \mathbf{N} is a nonlinear operator with noise terms.

$$\mathbf{L} = \frac{i}{2}(1 \pm \frac{\partial^2}{\partial\tau^2}) - \gamma \quad (12)$$

$$\mathbf{N} = i\phi^+\phi^2 + \xi_L + \sqrt{i}\xi_E\phi \quad (13)$$

The solution of the (11) can be approximated as.

$$\phi(\zeta + \Delta\zeta, \tau) \approx \exp\left(\frac{\Delta\zeta}{2}\mathbf{L}\right) \exp\left(\int_{\zeta'}^{\zeta'+\Delta\zeta} \mathbf{N}(\zeta')d\zeta'\right) \times \exp\left(\frac{\Delta\zeta}{2}\mathbf{L}\right)\phi(\zeta, \tau) \quad (14)$$

Similarly, (4b) can also be split into linear and nonlinear operator forms. In order to estimate $\phi(\zeta_{n+1})$ from $\phi(\zeta_n)$, following steps are followed according semi implicit midpoint method;

$$\bar{\phi}_n^{(0)} = \mathcal{F}^{-1}\left[\exp\left(\left(\frac{i}{2}(1 \pm k^2) - \gamma\right)\frac{\Delta\zeta}{2}\right)\mathcal{F}[\phi_n]\right] \quad (15a)$$

$$\bar{\phi}_n^{+(0)} = \mathcal{F}^{-1}\left[\exp\left(\left(\frac{-i}{2}(1 \pm k^2) - \gamma\right)\frac{\Delta\zeta}{2}\right)\mathcal{F}[\phi_n^+]\right] \quad (15b)$$

$$\begin{aligned} \bar{\phi}_n^{(i)} = \bar{\phi}_n^{(0)} &+ \frac{\Delta\zeta}{2}(i\bar{\phi}_n^{+(i-1)})(\bar{\phi}_n^{(i-1)})^2 \\ &+ \xi_L(\zeta_n) + \sqrt{i}\xi_E(\zeta_n)\bar{\phi}_n^{(i-1)} \end{aligned} \quad (16a)$$

$$\begin{aligned} \bar{\phi}_n^{+(i)} = \bar{\phi}_n^{+(0)} &+ \frac{\Delta\zeta}{2}(i\bar{\phi}_n^{(i-1)})(\bar{\phi}_n^{+(i-1)})^2 \\ &+ \xi_L^+(\zeta_n) + \sqrt{-i}\xi_E^+(\zeta_n)\bar{\phi}_n^{+(i-1)} \end{aligned} \quad (16b)$$

$$\phi_{n+1} = \mathcal{F}^{-1}\left[e^{\left(\frac{i}{2}(1 \pm k^2) - \gamma\right)\frac{\Delta\zeta}{2}}\mathcal{F}[2\bar{\phi}_n^{(4)} - \bar{\phi}_n^{(0)}]\right] \quad (17a)$$

$$\phi_{n+1}^+ = \mathcal{F}^{-1}\left[e^{\left(\frac{-i}{2}(1 \pm k^2) - \gamma\right)\frac{\Delta\zeta}{2}}\mathcal{F}[2\bar{\phi}_n^{+(4)} - \bar{\phi}_n^{+(0)}]\right] \quad (17b)$$

In the above equations, \mathcal{F} is the Fourier transform operator. In above mentioned equations $\phi_n(\phi_n^+)$ means $\phi(\zeta_n)(\phi^+(\zeta_n))$. A discretized ϕ and ϕ^+ in τ at $\zeta = 0$ as the initial condition is input in the above numerical method to get the field's evolution inside the optical fiber.

VI. CONCLUSION

We have provided a theoretical method for crosstalk analysis between strong signals carrying classical data and weak signals utilized for quantum communication tasks. We defined the crosstalk as the relative distortion of a weak optical pulse in the presence and absence of a classical communication link. Our comprehensive approach proves the robustness of the WDM method in integrating the quantum channel alongside the classical communication channel. Co-propagation is analyzed

in the C-band with a standard ITU 100 GHz spacing grid. Our results show that a separation of 2 ITU channels (2.39 nm) between a quantum- and the classical signal is sufficient and leads to negligible crosstalk. We have thus highlighted the capabilities of a powerful method which may be utilized to accelerate the integration and adoption of QKD systems.

Outlook- We used the “overlap” $\mathcal{C}(\zeta)$ as a means of quantifying the impact of classical data signals on a quantum communication link. This work can be further expanded to include more application-specific metrics like the quantum bit error rate instead of $\mathcal{C}(\zeta)$. Future work needs to identify the pulse duration sweet spot that can offer minimum crosstalk with a particular choice of WDM channel spacing. In addition, this formalism must be adapted to model Fock state propagation in the presence of classical signals that will help in understanding the crosstalk behavior of QKD using a single photon source when multiplexed with classical channels. Therefore, this work plays a significant role in feasibly cost-effectively scaling the quantum networks by utilizing existing telecom infrastructure.

REFERENCES

- [1] S. Pirandola, U. L. Andersen, L. Banchi, M. Berta, D. Bunandar, R. Colbeck, D. Englund, T. Gehring, C. Lupo, C. Ottaviani, *et al.*, “Advances in quantum cryptography,” *Advances in optics and photonics*, vol. 12, no. 4, pp. 1012–1236, 2020.
- [2] Y. Liu, W.-J. Zhang, C. Jiang, J.-P. Chen, C. Zhang, W.-X. Pan, D. Ma, H. Dong, J.-M. Xiong, C.-J. Zhang, *et al.*, “Experimental twin-field quantum key distribution over 1000 km fiber distance,” *Physical Review Letters*, vol. 130, no. 21, p. 210801, 2023.
- [3] A. Shamir, “How to share a secret,” *Communications of the ACM*, vol. 22, p. 612–613, nov 1979.
- [4] M. Hillery, V. Bužek, and A. Berthiaume, “Quantum secret sharing,” *Physical Review A*, vol. 59, p. 1829–1834, Mar. 1999.
- [5] A. Dutta and A. Pathak, “A short review on quantum identity authentication protocols: how would bob know that he is talking with alice?,” *Quantum Information Processing*, vol. 21, p. 369, 2022.
- [6] D. Gottesman and I. Chuang, “Quantum digital signatures,” *arXiv preprint quant-ph/0105032*, 2001.
- [7] P. D. Drummond and M. Hillery, *The quantum theory of nonlinear optics*. Cambridge University Press, 2014.
- [8] C. Agnesi, M. Avesani, A. Stanco, P. Villoresi, and G. Vallone, “All-fiber self-compensating polarization encoder for quantum key distribution,” *Optics letters*, vol. 44, no. 10, pp. 2398–2401, 2019.
- [9] J. Jin, J.-P. Bourgoin, R. Tannous, S. Agne, C. J. Pugh, K. B. Kuntz, B. L. Higgins, and T. Jennewein, “Genuine time-bin-encoded quantum key distribution over a turbulent depolarizing free-space channel,” *Optics express*, vol. 27, no. 26, pp. 37214–37223, 2019.
- [10] E. Diamanti, H. Takesue, C. Langrock, M. M. Fejer, and Y. Yamamoto, “100 km differential phase shift quantum key distribution experiment with low jitter up-conversion detectors,” *Opt. Express*, vol. 14, pp. 13073–13082, Dec 2006.
- [11] N. K. Pathak, S. Chaudhary, Sangeeta, and B. Kanseri, “Phase encoded quantum key distribution up to 380 km in standard telecom grade fiber enabled by baseline error optimization,” *Scientific Reports*, vol. 13, no. 1, p. 15868, 2023.
- [12] K. Tamaki, H.-K. Lo, C.-H. F. Fung, and B. Qi, “Phase encoding schemes for measurement-device-independent quantum key distribution with basis-dependent flow,” *Phys. Rev. A*, vol. 85, p. 042307, Apr 2012.
- [13] C. H. Bennett and G. Brassard, “Quantum cryptography: Public key distribution and coin tossing,” *Theoretical Computer Science*, vol. 560, p. 7–11, Dec. 2014.
- [14] S. Wiesner, “Conjugate coding,” *SIGACT News*, vol. 15, p. 78–88, jan 1983.
- [15] D. J. Bernstein, *Introduction to post-quantum cryptography*, pp. 1–14. Berlin, Heidelberg: Springer Berlin Heidelberg, 2009.
- [16] I. Devetak, “The private classical capacity and quantum capacity of a quantum channel,” *IEEE Transactions on Information Theory*, vol. 51, no. 1, pp. 44–55, 2005.
- [17] Y. Mao, B.-X. Wang, C. Zhao, G. Wang, R. Wang, H. Wang, F. Zhou, J. Nie, Q. Chen, Y. Zhao, *et al.*, “Integrating quantum key distribution with classical communications in backbone fiber network,” *Optics express*, vol. 26, no. 5, pp. 6010–6020, 2018.
- [18] T. J. Xia, D. Z. Chen, G. A. Wellbrock, A. Zavriyev, A. C. Beal, and K. M. Lee, “In-band quantum key distribution (qkd) on fiber populated by high-speed classical data channels,” in *Optical Fiber Communication Conference*, p. OTuJ7, Optical Publishing Group, 2006.
- [19] I. Choi, Y. R. Zhou, J. Dynes, Z. Yuan, A. Klar, A. Sharpe, A. Plews, M. Lucamarini, C. Radig, J. Neubert, *et al.*, “First quantum secured 10-gb/s dwdm transmission over the same installed fibre,” in *2014 The European Conference on Optical Communication (ECOC)*, pp. 1–3, IEEE, 2014.
- [20] L.-J. Wang, K.-H. Zou, W. Sun, Y. Mao, Y.-X. Zhu, H.-L. Yin, Q. Chen, Y. Zhao, F. Zhang, T.-Y. Chen, *et al.*, “Long-distance copropagation of quantum key distribution and terabit classical optical data channels,” *Physical Review A*, vol. 95, no. 1, p. 012301, 2017.
- [21] J. F. Dynes, W. W. Tam, A. Plews, B. Fröhlich, A. W. Sharpe, M. Lucamarini, Z. Yuan, C. Radig, A. Straw, T. Edwards, *et al.*, “Ultra-high bandwidth quantum secured data transmission,” *Scientific reports*, vol. 6, no. 1, p. 35149, 2016.
- [22] T. A. Eriksson, T. Hirano, B. J. Putnam, G. Rademacher, R. S. Luís, M. Fujiwara, R. Namiki, Y. Awaji, M. Takeoka, N. Wada, *et al.*, “Wavelength division multiplexing of continuous variable quantum key distribution and 18.3 tbit/s data channels,” *Communications Physics*, vol. 2, no. 1, p. 9, 2019.
- [23] P. Gavignet, E. Pincemin, F. Herviou, Y. Loussouarn, F. Mondain, A. Grant, L. Johnson, R. I. Woodward, J. F. Dynes, B. Summers, *et al.*, “Co-propagation of qkd & 6 tb/s (60x100g) dwdm channels with 17 dbm total wdm power in single and multi-span configurations,” *Journal of Lightwave Technology*, 2023.
- [24] F. Honz, F. Prawits, O. Alia, H. Sakr, T. Bradley, C. Zhang, R. Slavík, F. Poletti, G. Kanellos, R. Nejabati, *et al.*, “First demonstration of 25λ × 10 gb/s c+1 band classical/dv-qkd co-existence over single bidirectional fiber link,” *Journal of Lightwave Technology*, vol. 41, no. 11, pp. 3587–3593, 2023.
- [25] S. J. Carter, “Quantum theory of nonlinear fiber optics: Phase-space representations,” *Phys. Rev. A*, vol. 51, pp. 3274–3301, Apr 1995.
- [26] P. D. Drummond and J. F. Corney, “Quantum noise in optical fibers. i. stochastic equations,” *JOSA B*, vol. 18, no. 2, pp. 139–152, 2001.
- [27] P. D. Drummond and S. J. Carter, “Quantum-field theory of squeezing in solitons,” *JOSA B*, vol. 4, no. 10, pp. 1565–1573, 1987.
- [28] G. P. Agrawal, *Fiber-optic communication systems*. John Wiley & Sons, 2012.
- [29] S. Wang, W. Chen, J.-F. Guo, Z.-Q. Yin, H.-W. Li, Z. Zhou, G.-C. Guo, and Z.-F. Han, “2 ghz clock quantum key distribution over 260 km of standard telecom fiber,” *Optics letters*, vol. 37, no. 6, pp. 1008–1010, 2012.
- [30] R. Sax, A. Boaron, G. Boso, S. Atzeni, A. Crespi, F. Grünenfelder, D. Rusca, A. Al-Saadi, D. Bronzi, S. Kupijai, *et al.*, “High-speed integrated qkd system,” *Photonics Research*, vol. 11, no. 6, pp. 1007–1014, 2023.
- [31] W. Li, L. Zhang, H. Tan, Y. Lu, S.-K. Liao, J. Huang, H. Li, Z. Wang, H.-K. Mao, B. Yan, *et al.*, “High-rate quantum key distribution exceeding 110 mb s⁻¹,” *Nature Photonics*, vol. 17, no. 5, pp. 416–421, 2023.
- [32] D. Subacius, A. Zavriyev, and A. Trifonov, “Backscattering limitation for fiber-optic quantum key distribution systems,” *Applied Physics Letters*, vol. 86, no. 1, p. 011103, 2005.
- [33] H. Ibarra-Villalon, O. Pottiez, A. Gómez-Vieyra, J. Lauterio-Cruz, and Y. Bracamontes-Rodríguez, “Numerical approaches for solving the nonlinear schrödinger equation in the nonlinear fiber optics formalism,” *Journal of Optics*, vol. 22, no. 4, p. 043501, 2020.
- [34] H. Ibarra-Villalon, O. Pottiez, A. Gómez-Vieyra, J. Lauterio-Cruz, and Y. Bracamontes-Rodríguez, “Embedded split-step methods optimized with a step size control for solving the femtosecond pulse propagation problem in the nonlinear fiber optics formalism,” *Physica Scripta*, vol. 96, no. 7, p. 075502, 2021.
- [35] M. J. Werner and P. D. Drummond, “Robust algorithms for solving stochastic partial differential equations,” *Journal of computational physics*, vol. 132, no. 2, pp. 312–326, 1997.